Rigorous Simulation Study of a Novel Non-Volatile Magnetic Flip-Flop

Thomas Windbacher, Hiwa Mahmoudi, Viktor Sverdlov, and Siegfried Selberherr
Institute for Microelectronics, TU Wien, Gußhausstraße 27–29/E360, A–1040 Wien, Austria
Email: {windbacher | mahmoudi | sverdlov | selberherr}@iue.tuwien.ac.at

***Abstract*—The ever increasing demand in fast and cheap bulk memory as well as electronics in general has driven the scaling efforts in CMOS since its very beginnings. Today, pushing the limits of integration density is still a major concern, but gradually power efficient computing gains more and more interest. A possible way to reduce power consumption is to introduce non-volatility into the devices. Thus power is consumed only, when information is written or read out, while the rest of the time the devices preserve the information with out any power demand. In this work we propose a novel non-volatile magnetic flip-flop which shifts the actual logic operation from the electric signal domain to the magnetic domain, operating via constructive and destructive superposition of spin waves generated by the spin transfer torque effect. Furthermore we carried out a rigorous simulation study for three different device sizes and found them operational between $\approx 4 \times 10^{10}\,\mathrm{A/m^2}$ and $\approx 10^{12}\,\mathrm{A/m^2}$ at switching times from tens of nanoseconds to picoseconds.**

I. Introduction

As device dimensions shrank below 100 nm, leakage currents for the first time increased to a level at which the static power consumption overtook the dynamic power loss [1]. A possibility to resolve this problem and to increase power efficiency in general is to introduce non-volatility into devices. Thus power is consumed only when information is written or read out, while the rest of the time the devices can be turned off entirely enabling true instant on applications. Even though many circuit designs have been proposed to achieve this goal, e.g., [2], the non-volatility is commonly introduced by ancillary devices like magnetic tunnel junctions (MTJs), merely holding the information without any further functionality. The logic operations are carried out in CMOS technology adding complexity because of the need for converting the information between resistance state and voltage or current signals every time data is saved or read.

II. Idea and Operation Principle

We propose a novel non-volatile magnetic flip-flop which not only holds the information in the magnetic domain but actually carries out the logic operations via spin waves enabling denser and simpler layouts as well as harvesting the beneficial features related to spintronics. This is achieved by three magnetic stacks, each including a spin tunnel barrier (two spin valve stacks for input and one MTJ stack for readout) sharing a common free magnetic layer (see Fig. 1). The logic information is stored via the magnetic orientation of the free layer and the polarity of the input pulses is mapped to logic "0" and "1", respectively.

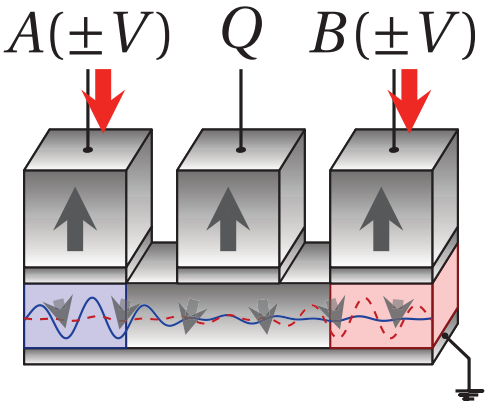

Fig. 1. Scheme of the proposed non-volatile magnetic flip-flop. A and B denote the inputs for the two spin valve stacks and Q denotes the output for the readout MTJ stack. The common shared free layer carries and transmits the generated spin waves. The spin waves either posses no phase shift (identical pulse polarities) or are 180° phase shifted (opposing pulse polarities). The resulting constructive or destructive superposition of the two spin waves either writes a given magnetization orientation in the common free layer or holds its state.

A current pulse to one of the input stacks (A or B) exerts a spin transfer torque on the magnetization in the corresponding free layer region of the input stack and generates a spin wave which travels through the common free layer heading to its opposite end, where it is reflected and moves back, gets reflected, and pushed again and so on [3]. During this kind of oscillating spin wave motion, the localized magnetic moments in the common free layer are excited and their precessional motions build up, until they eventually pass the energy barrier separating its two stable states and relax into the other stable state fast. If two synchronous current pulses are applied to the input stacks A and B, two moving spin waves are generated, which either superimpose constructively (current pulses exhibit same polarity and thus same torque orientation) or destructively (current pulses exhibit opposing polarities and thus opposing spin torque orientations). Thus, two sufficiently high and long pulses with identical polarity either write logic "0" or "1" into the common free layer, while two pulses with opposing polarities cancel each other and the initial magnetization state is held; representing a sequential logic function needed for flip-flop logic (cf. Tab. I). If one of the inputs is inverted the resulting logic sets or resets the held state, when the input signals are opposing and holds its state for identical input polarities, which corresponds to RS flip-flop logic without forbidden

978-1-4673-5736-4/13/$31.00 ©2013 IEEE

input combinations (see Tab. II and [4]).

TABLE I. SEQUENTIAL LOGIC FUNCTION OF THE PROPOSED NON-VOLATILE MAGNETIC FLIP-FLOP. THE PULSE POLARITIES APPLIED TO THE INPUTS A AND B AT TIME STEP $i-1$ RESULT IN A RESISTANCE STATE Q AT TIME STEP i.

A	B	$Q(i)$
0	0	0
0	1	$Q(i-1)$
1	0	$Q(i-1)$
1	1	1

TABLE II. INVERTING ONE OF THE INPUT PULSES OR ONE OF THE POLARIZER STACKS' MAGNETIZATION ORIENTATIONS LEADS TO A LOGIC FUNCTION KNOWN AS RS FLIP-FLOP, BUT WITHOUT FORBIDDEN INPUT COMBINATIONS.

$R/\bar{A}$	S/B	$Q(i)$
0	0	$Q(i-1)$
0	1	1
1	0	0
1	1	$Q(i-1)$

III. SIMULATION SETUP

The flip-flops operational functionality was tested with an extensive simulation study [5] assuming 10 nm, 20 nm, and 30 nm wide; 40 nm, 80 nm, and 120 nm long; and 3 nm thick common free layers; exhibiting a magnetization saturation of 4×10^5 A/m; an out-of-plane uni-axial crystal anisotropy of 10^5 J/m^3; an exchange constant of 2×10^{-11} J/m; and a spin current polarization of 0.3. Furthermore, we assume that the input stacks of A and B consist of an anti-ferromagnetic layer stack with negligible influence on the local magnetic field. The micromagnetic dynamics of the flip-flop is governed by the Landau-Lifshitz-Gilbert equation [6], [7]:

$$\frac{d\vec{m}}{dt} = \gamma\left(-\vec{m}\times\vec{H}_{eff}+\alpha\left(\vec{m}\times\frac{d\vec{m}}{dt}\right)+ + \beta\epsilon\left(\vec{m}\times\vec{p}\times\vec{m}-\epsilon'\vec{m}\times\vec{p}\right)\right), \quad (1)$$

$\vec{m}$ denotes the reduced magnetization, $\gamma = 2.211\times10^5\, m/As$ the Gilbert gyromagnetic ratio, $\alpha = 0.01$ the dimensionless damping constant, $\vec{H}_{eff}$ the effective field in A/m, and $\vec{p}$ the unit polarization direction of the polarized current. The last term in (1) describes the spin transfer torque [8], [9] contribution including a non-adiabatic contribution of $\epsilon' = 0.1$ [10]. The term $\beta\epsilon$ is given by:

$$\beta\epsilon = \frac{\hbar}{\mu_0 e}\frac{J}{lM_s}\frac{P\Lambda^2}{(\Lambda^2+1)+(\Lambda^2-1)(\vec{m}\cdot\vec{p})}, \quad (2)$$

$\hbar$ denotes the Planck constant, μ_0 the permittivity of vacuum, e the electron charge, J the applied current density, l the free layer thickness, M_s the magnetization saturation, P the polarization, and $\Lambda = 2$ a parameter handling geometrical non-idealities. Furthermore, $\vec{H}_{eff}$ is calculated from the functional derivative of the free energy density containing uni-axial anisotropy, exchange, and demagnetization contributions [11].

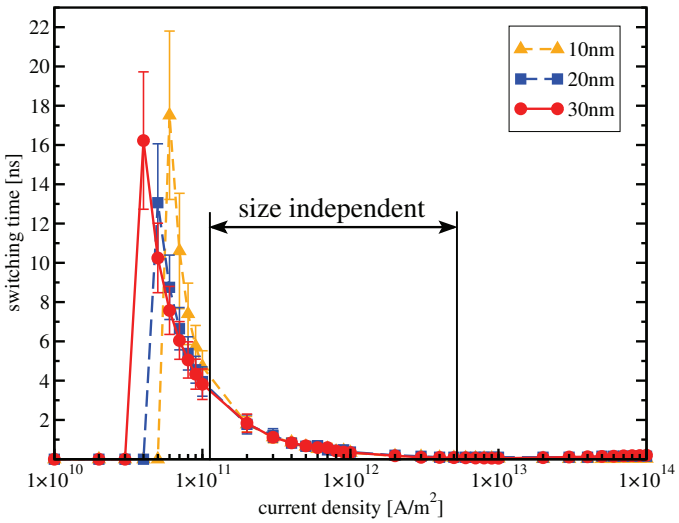

Fig. 2. Averaged switching speed as a function of applied current density and size for identical input pulses and opposing common free layer magnetization. Smaller sizes need higher frequencies for excitation, requiring higher torques and thus higher current densities.

The shown current densities state an average over ±5% of the respective current density and several simulations (see Fig. 2 and Fig. 4). The error bars depict an error range of $\pm3\times\sigma$. Switching time is defined as the time from the onset of the current pulse until 80% of the final magnetization orientation is reached. In the case of opposing pulses - the magnetization state must be held - for a reliable flip-flop operation the reduced magnetization $\vec{m}$ must relax back to its initial orientation, when the pulse is over. For instance, starting with an initial magnetization state along the positive z-axis, the precessional motions must not cross the xy-plane ($m_z > 0$). Otherwise the precessional motions cross the state separating energy barrier and the final magnetization state starts to depend on the pulse length or in other words, this is the point where the initial information is lost.

IV. RESULTS

One can see in Fig. 2 that for the set and reset operation (identical input pulses) the flip-flop behaves similarly to a single magnetic stack (in the beginning high switching times at low current densities followed by a fast drop in switching times, when the current density is increased) and that for smaller devices initially higher current densities are needed for switching. This can be explained as follows: For shorter shared free layers higher frequencies are needed to excite the precessions required for switching, which in turn demands higher spin transfer torques and by that higher current densities. For a pulse length of 20 ns switching starts at 4×10^{10} A/m^2 (16 ± 3.5 ns), 5×10^{10} A/m^2 (13 ± 3 ns), and 6×10^{10} A/m^2 (17.5 ± 4.3 ns) for 30 nm, 20 nm, and 10 nm, respectively. Interestingly, the switching speed becomes almost size independent around $\approx10^{11}$ A/m^2 until $\approx5\times10^{12}$ A/m^2 and the found minimum switching times are between ≈ 20 ps and ≈ 100 ps.

Fig. 3 depicts the space average reduced magnetization component $< m_z(t) >$ and the total energy as a function of

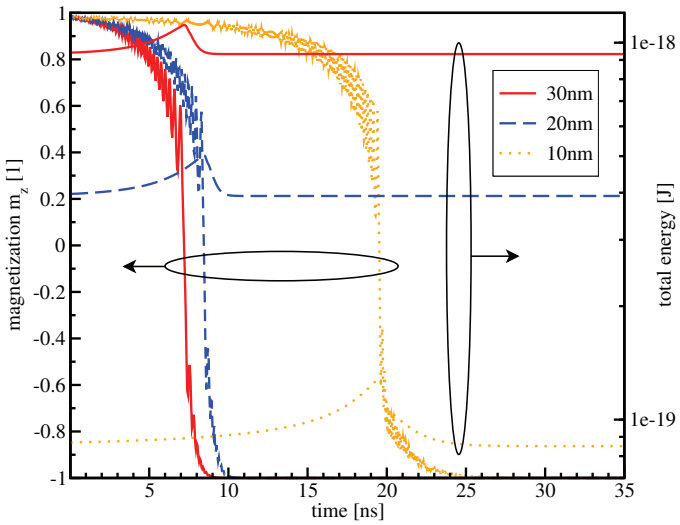

Fig. 3. z-component of the total free layer magnetization and total energy of the system as a function of time at $6\times10^{10}\,\mathrm{A/m^2}$ and equal polarities.

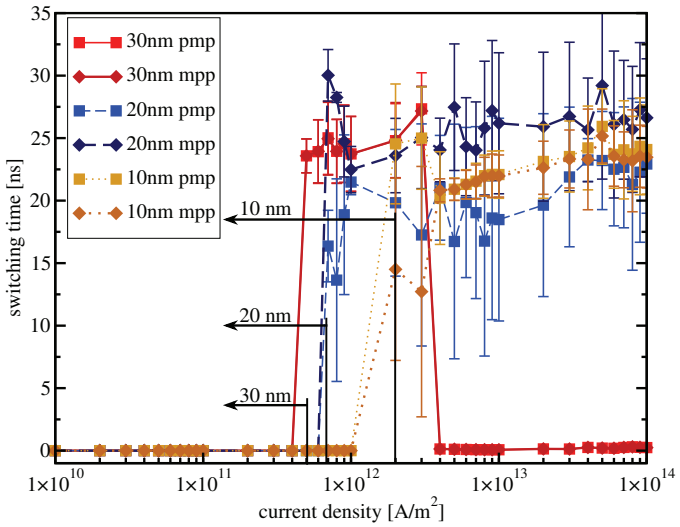

Fig. 4. Switching as a function of size and applied current densities for opposing input pulses. The arrows denote the region for which the normalized magnetization component m_z during the precessional motions stays above 0 and the operation result does not depend on the pulse duration.

time at $6\times10^{10}\,\mathrm{A/m^2}$ and equal pulse polarities. Analogously to a single stack the precessional motion of the local magnetization starts to build up until it passes the energy barrier separating its two stable states and relaxes fast into the new stable state.

In order to ensure a safe hold operation (opposing input polarities) there must not be a switching event. This holds true for current densities below $2\times10^{12}\,\mathrm{A/m^2}$ and 10 nm width, $7\times10^{11}\,\mathrm{A/m^2}$ and 20 nm width, and $5\times10^{11}\,\mathrm{A/m^2}$ and 30 nm length (as shown in Fig. 4). Close to the respective current densities the opposing spin waves from the two input stacks A and B do not compensate each other entirely and oscillatory motions start to build up. Above the given boundaries the oscillations can become so strong that they cross the xy-plane and the initial magnetization orientation

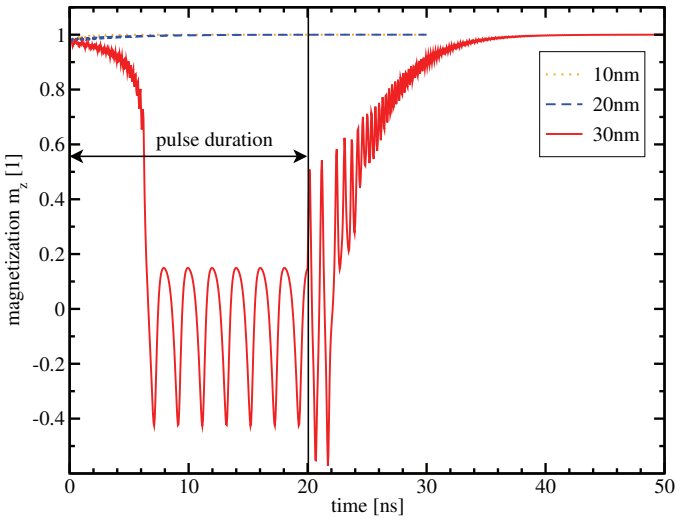

Fig. 5. z-component of the total free layer magnetization as a function of time at $5\times10^{11}\,\mathrm{A/m^2}$ for opposing pulse polarities. One can see for 30 nm oscillations are developed because of the longer wave path.

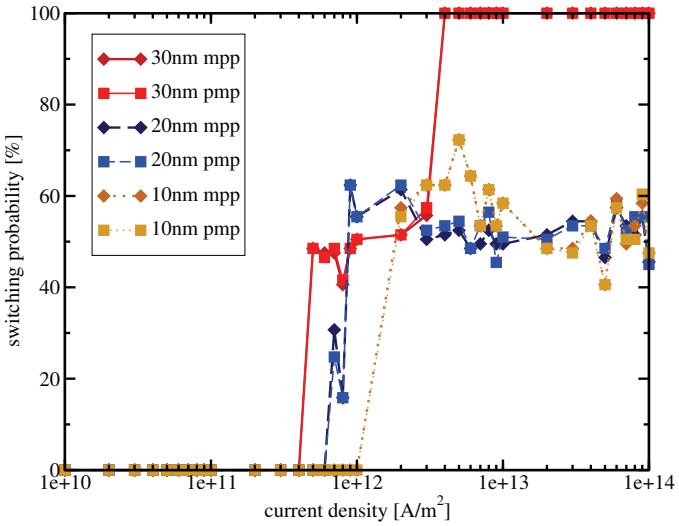

Fig. 6. Switching probabilities as a function of size and applied current densities for opposing input pulses. Regions with 0% switching probability confirm the persistence of the initial magnetization state while regions exhibiting ≈ 50% switching probability indicate the loss of the initial information due to strong precessional motions of the localized magnetization. The data points for 30 nm and 100% switching probability feature no oscillations, but only direct relaxations into the other state consistent to the switching times in Fig. 4.

holding the information is lost. This can also be seen in Fig. 5 where the z-component of the reduced magnetization $m_z(t)$ as a function of time for different layer sizes and opposing input polarities is shown. While for 10 nm and 20 nm only the damped motion back to its initial equilibrium position is visible, at 30 nm strong oscillations start around 7 ns and persist, until the input pulses are turned of at 20 ns. Since these oscillations cross the xy-plane the initial information may be lost and the magnetization state after relaxation depends on the pulse duration. Due to the geometrical dependencies for the excited spin waves the oscillation frequencies as well as the required (onset)

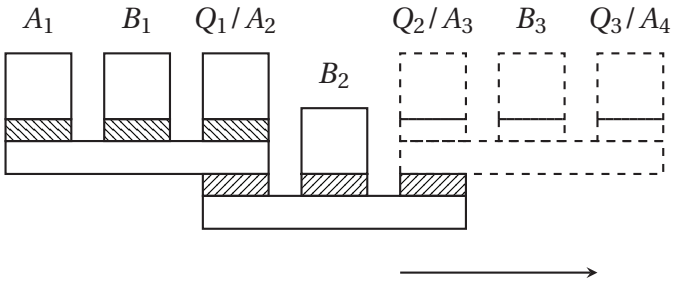

Fig. 7. Side view of a shift register topology enabling information transport via spin transfer torque. Either the first level (A_1,B_1,Q_2/A_3,B_3,$\cdots$, first clock signal Clk_1) is powered or the second level is active (Q_1/A_2,B_2,$\cdots$, second clock Clk_2) passing the information stored in the shared free layers between the subsequent flip-flops [12].

current densities for their excitation differ for the different shared free layer sizes.

Fig. 6 depicts the switching probabilities for opposing pulses and shows that for 30 nm, when the current density increases, initially there is no switching, followed by a region where strong resonant oscillations take place. At even higher current densities the direct magnetization flipping without oscillations is observed. This is consistent with the rapid switching time drop for 30 nm seen in Fig. 4. Deviations from the $\approx 50\%$ switching probability stem from the different excited oscillation modes and their related oscillation paths as well as the pulse length (for short enough pulses the initial magnetization information is not entirely destroyed).

Looking closer at the switching times one can see for 10 nm and especially 20 nm a mismatch in the relaxation times of the mpp and pmp branch (mpp stands for $A = \downarrow$ (0), $B = \uparrow$ (1), and $Q(i-1) = \uparrow$ while pmp denotes $A = \uparrow$ (1), $B = \downarrow$ (0), and $Q(i-1) = \uparrow$ with respect to the z-axis). These two combinations promote two different precessional motions (clockwise and counter clockwise) with respect to the z-axis leading to differing precessional paths and relaxation (switching) times.

V. Discussion

The proposed non-volatile magnetic flip-flop is very space efficient compared to CMOS flip-flops requiring eight transistors (non clocked) or twelve transistors (clocked) for a classical RS flip-flop [4]. It is more efficient as compared to hybrid MTJ/CMOS circuits requiring seven transistors and two magnetic tunnel junction memory elements for a flip-flop as proposed in [2]. Instead only three magnetic stacks (spin valve and/or MTJ) exhibiting a shared free layer are needed and there are no forbidden input combinations ($R = S = 1 \rightarrow Q = \bar{Q} = 0$ cf. Tab. II) giving more freedom to circuit and logic design.

The flip-flop is also very attractive for large scale integration because of its CMOS compatibility and stack friendly topology. In [12] we apply the proposed flip-flop for a non-volatile shift register with an extremely dense layout allowing further reduction of the required space (cf. Fig. 7).

Finally, the strong and stable precessional motions in the xy-plane for the hold operation at elevated current densities could be utilized for large gain spin torque nano-oscillators [13], [14], [15].

VI. Conclusion

The non-volatile magnetic flip-flops presented were found to be operational between $\approx 4 \times 10^{10}\,\mathrm{A/m^2}$ and $\approx 10^{12}\,\mathrm{A/m^2}$. The switching speed depends on the applied current density and is in the range of tens of nanoseconds to picoseconds (see Fig. 2 to Fig. 5). The proposed topology reduces integration space, it is stack friendly and thus extendable to more complex circuits, e.g a shift register [12]. A significant advantage of the shown flip-flop is that it stays CMOS compatible. A possible application as spin torque nano-oscillator is also appealing.

Acknowledgment

This work is supported by the European Research Council through the grant #247056 MOSILSPIN.

References

[1] N. Kim, T. Austin, D. Baauw, T. Mudge, K. Flautner, J. Hu, M. Irwin, M. Kandemir, and V. Narayanan, "Leakage current: Moore's law meets static power," *Computer*, vol. 36, no. 12, pp. 68–75, 2003.

[2] W. Zhao, L. Torres, Y. Guillemenet, L. V. Cargnini, Y. Lakys, J.-O. Klein, D. Ravelosona, G. Sassatelli, and C. Chappert, "Design of MRAM based logic circuits and its applications," in *ACM Great Lakes Symposium on VLSI*, 2011, pp. 431–436.

[3] R. Hertel, *Guided Spin Waves*. John Wiley & Sons, Ltd, 2007.

[4] U. Tietze and C. Schenk, *Electronic Circuits — Handbook for Design and Applications*, 2nd ed. Springer, 2008, no. 12.

[5] M. Donahue and D. Porter, "OOMMF user's guide," Interagency Report NISTIR 6376, version 1.0.

[6] T. Gilbert, "A lagrangian formulation of the gyromagnetic equation of the magnetization field." *Phys. Rev.*, vol. 100, p. 1243, 1955.

[7] H. Kronmüller, *General Micromagnetic Theory*. John Wiley & Sons, Ltd, 2007.

[8] J. Xiao, A. Zangwill, and M. D. Stiles, "Boltzmann test of Slonczewski's theory of spin-transfer torque," *Phys. Rev. B*, vol. 70, p. 172405, Nov 2004.

[9] J. Slonczewski, "Current-driven excitation of magnetic multilayers," *Journal of Magnetism and Magnetic Materials*, vol. 159, no. 1–2, pp. L1 – L7, 1996.

[10] A. V. Khvalkovskiy, K. A. Zvezdin, Y. V. Gorbunov, V. Cros, J. Grollier, A. Fert, and A. K. Zvezdin, "High domain wall velocities due to spin currents perpendicular to the plane," *Phys. Rev. Lett.*, vol. 102, p. 067206, Feb 2009.

[11] J. E. Miltat and M. J. Donahue, *Numerical Micromagnetics: Finite Difference Methods*. John Wiley & Sons, Ltd, 2007.

[12] T. Windbacher, H. Mahmoudi, V. Sverdlov, and S. Selberherr, "Novel MTJ-based shift register for non-volatile logic applications," *NANOARCH*, 2013.

[13] Z. Zeng, G. Finocchio, B. Zhang, P. K. Amiri, J. A. Katine, I. N. Krivorotov, Y. Huai, J. Langer, B. Azzerboni, K. L. Wang, and H. Jiang, "Ultralow-current-density and bias-field-free spin-transfer nano-oscillator," *Sci. Rep.*, vol. 3, pp. 1–5, Mar. 2013.

[14] S. Ikeda, K. Miura, H. Yamamoto, K. Mizunuma, H. D. Gan, M. Endo, S. Kanai, J. Hayakawa, F. Matsukura, and H. Ohno, "A perpendicular-anisotropy CoFeB-MgO magnetic tunnel junction," *Nat Mater*, vol. 9, pp. 721–724, Aug. 2010.

[15] M. Tsoi, A. G. M. Jansen, J. Bass, W.-C. Chiang, M. Seck, V. Tsoi, and P. Wyder, "Excitation of a magnetic multilayer by an electric current," *Phys. Rev. Lett.*, vol. 80, pp. 4281–4284, May 1998.